ORIGINAL PAPER

Experimental study on the shear creep of rock-like materials with cracks

Liangxiao Xiong[1,2] · Haijun Chen[3] · Haiyang Yuan[4] · Zhongyuan Xu[5]

Abstract

In this study, the shear creep of intact rock-like samples and rock-like samples with cracks are tested in a laboratory. The effects of shear stress magnitude, crack inclination, and crack length on the instantaneous shear displacement, shear creep displacement, long-term shear strength, and fracture morphology are analyzed. Based on the software element proposed by previous studies according to the fractional derivative theory, a nonlinear shear rheological model of the rock-like samples with cracks is proposed by combining existing element models. The following results are shown: (1) With an increase in horizontal shear stress, the shear creep displacement and average shear creep displacement rate of the specimen increase when the fracture dip angle, fracture length, and normal stress are the same. (2) When the crack length, normal stress, shear stress, and creep time remain the same, with the crack inclination increasing from 0 to 90°, the shear creep displacement first increases and then decreases, and the long-term strength first decreases, and then increases. (3) When the normal stress and tangential stress are the same, and the crack dip angle is constant, an increase in the crack length increases the instantaneous shear displacement and shear creep displacement and decreases the long-term shear strength. (4) During the shear creep test, the cracks first appear at the tip of the prefabricated crack and then extend to the contact point between the specimen and the horizontally loaded plate.

Responsible Editor: Zeynal Abiddin Erguler

✉ Liangxiao Xiong
  xionglx1982@126.com

  Haijun Chen
  hjchen@nhri.cn

  Haiyang Yuan
  1045919790@qq.com

  Zhongyuan Xu
  zyxu@swjtu.edu.cn

1 School of Civil Engineering and Architecture, East China Jiaotong University, Nanchang 330013, China

2 State Key Laboratory of Geohazard Prevention and Geoenvironment Protection, Chengdu University of Technology, Chengdu University of Technology, Chengdu 610059, Sichuan Province, China

3 Geotechnical Engineering Department, Nanjing Hydraulic Research Institute, Nanjing 210029, China

4 College of Environment and Civil Engineering, Chengdu University of Technology, Chengdu 610059, China

5 Faculty of Geosciences and Environmental Engineering, Southwest Jiaotong University, Chengdu 611756, China

Introduction

Rheology is an important mechanical property of rocks. Many studies have conducted numerous experimental studies on the rheological properties of rocks. Structural planes often exist in practical engineering rock masses. Thus, the shear rheological properties of structural planes are important in the long-term stability of practical rock mass engineering.

Only a few studies have conducted experimental research on the shear rheological properties of structural planes. Shen and Zhu (2004) and Shen and Zhang (2008) studied the creep of regularly dentate discontinuities under biaxial stresses and found that the Burgers model could reflect the creep of discontinuities. Xu and Yang (2005) conducted a shear rheology experiment on unfilled jointed rock specimens from a huge underground cave in Longtan Hydropower Station. The comparison between the shear rheology model and experimental results showed that their proposed nonlinear shear rheology model was accurate and reasonable. Yang et al. (2007) conducted shear rheology experiments on shale from the Longtan Hydropower Project,
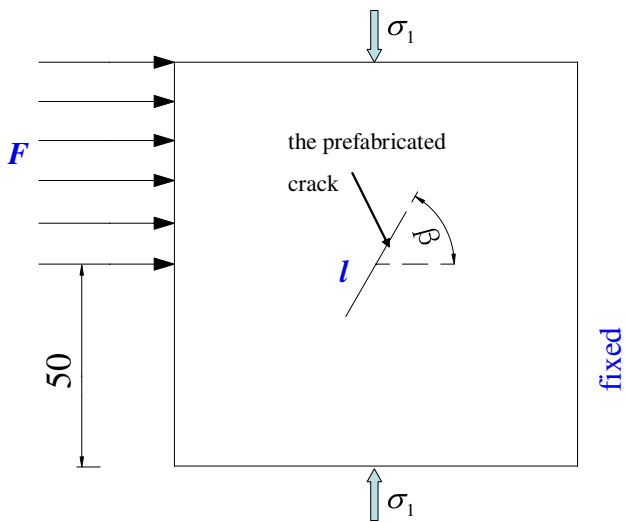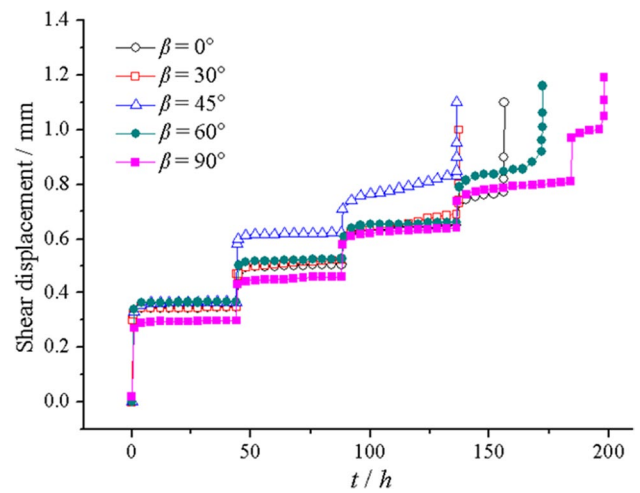
Fig. 1 Schematic diagram of direct shear creep test for specimens with prefabricated cracks (unit: mm)

Fig. 2 The shear creep test curves of the specimens when the crack length is 40 mm for different inclined angles of the cracks

and their comparison between the rheological model and their experimental results showed that the proposed rheological model worked reasonably well. Chen et al. (2008) found that the creep deformation of the structural face contains many elements of instantaneous elastic, instantaneous plastic, and viscoelastic and viscoplastic deformations. Li et al. (2008) conducted shear creep tests on the weak structural plane in sandstone with different water contents, and the results showed that the influence of water content on the shear creep deformation of a weak structural plane is significant. Yan et al. (2009) conducted shear rheology tests to study the elastic-viscoplastic behavior of marble rock joints from the Jinping Hydraulic Power Station, and their comparison between the model and test results showed that the proposed rheological model was reasonable. Shen and Zhang (2010) conducted shear creep tests for marble samples with greenschist discontinuities, and their results showed that the creep curves have three stages. Zhang et al. (2010) conducted shear creep experiments on sandstone with a weak plane, and
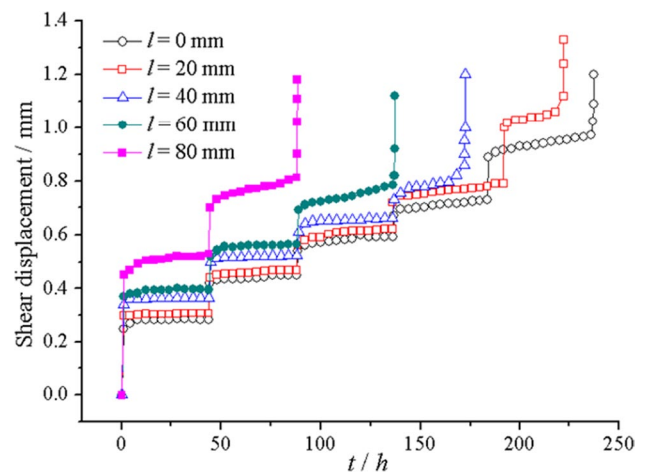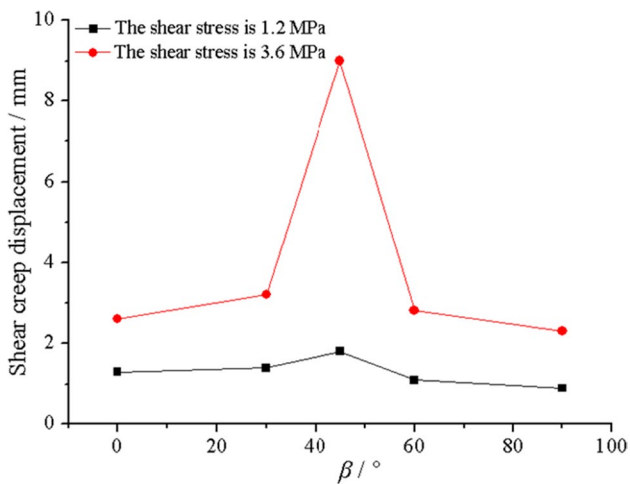
their results showed that the creep rate of the rock increased with an increase in the shear stress. Zhang et al. (2011a) conducted shear creep tests of dentate discontinuities under different normal stresses to study the creep of discontinuities with different slope ratios, and their results showed that steady creep does not exist. Zhang et al. (2011b) tested marble samples with weak structural planes using a multistage loading shear rheological method. Zhang et al. (2012) conducted shear tests and shear creep tests on regular jagged discontinuities with different angles and under different stresses and found that the modified Burger model is consistent with the shear creep test results of the structural plane. They found that the nonstationary shear creep model is more consistent with the experimental data than the stationary shear creep model. Shen et al. (2012) conducted laboratory shear creep tests on cement mortar specimens under

Table 1 The shear creep test samples

Specimen no	Crack length (mm)	Inclined angle of crack (°)
# S4-A0	40	0
# S4-A30	40	30
# S4-A45	40	45
# S4-A60	40	60
# S4-A90	40	90
# S2-A60	20	60
# S6-A60	60	60
# S8-A60	80	60

Fig. 3 Shear creep test curves of the specimens when the crack dip angle is 60° for five different crack lengths

Fig. 4 The change of the shear creep displacement of the specimen with cracks with the crack dip angle β when the crack length is 40 mm

different normal stresses. Their results showed that the long-term strength of structural planes obtained using transition creep, isochronal curve, and first inflection point methods were inconsistent. They found that marble samples with weak greenschist structural planes showed features of brittle failure. Jia et al. (2018) conducted laboratory shear creep tests on undisturbed rock discontinuities from Baihetan Hydropower Station, and the test curves of the rock discontinuity showed transient, steady-state, and accelerated creep stages.

When the above studies tested the shear rheological properties of the structural plane, the structural plane was often throughgoing. Moreover, the upper and lower rock blocks were separated, and the structural plane was horizontal. In actual rock mass engineering, the structural plane may not be throughgoing, and there is an angle between the structural plane and the horizontal shear direction. This study mainly conducted laboratory shear creep tests on intact rock-like samples and rock-like samples with cracks. In addition, the effects of the shear stress level, crack inclination, and crack length on the instantaneous shear displacement, shear creep displacement, long-term shear strength, and fracture morphology are analyzed.

Test principle

Sample preparation

The direct shear creep characteristics of artificial rock-like samples with cracks were tested. The rock-like samples were made of cement mortar. No. 425 Portland cement, medium standard sand, and a water/cement ratio of 0.65 were used. The sample was a 100 mm long × 100 mm wide × 100 mm high cubic sample. The inclined angle β of the prefabricated

fissures is the angle between the prefabricated crack and the horizontal, and five inclined angles were tested β: 0°, 30°, 45°, 60°, and 90°. The lengths l of the prefabricated fissures were 20 mm, 40 mm, 60 mm, and 80 mm. A schematic diagram of the direct shear creep test for specimens with prefabricated cracks is shown in Fig. 1.

Cement mortar was poured, vibrated, and compacted in a 100 mm high × 100 mm long × 100 mm wide test mold. A plastic sheet was inserted into the cement mortar after 12 h and removed after 12 h to form a prefabricated empty crack in the sample.

Instantaneous shear test

After curing the specimen for 28 days, three intact specimens were used for the instantaneous shear test to determine their instantaneous shear strength, providing a basis for determining the shear stress magnitude of the shear creep test. During the instantaneous shear test, the axial load is applied to the specimen at a speed of 5 kN/s. When the axial load reaches the predetermined value, it is maintained constant. Subsequently, the horizontal shear load is applied to the specimen at a loading rate of 5 kN/s until the specimen fails.

Through instantaneous shear test, the friction angle of the intact rock sample is 40.2°, and its cohesion is 6.69 MPa.

Shear creep test

The shear creep test was conducted on a shear rheological testing machine. When conducting the shear creep test on the intact specimen and the specimen with prefabricated cracks, the step-by-step incremental loading is adopted.
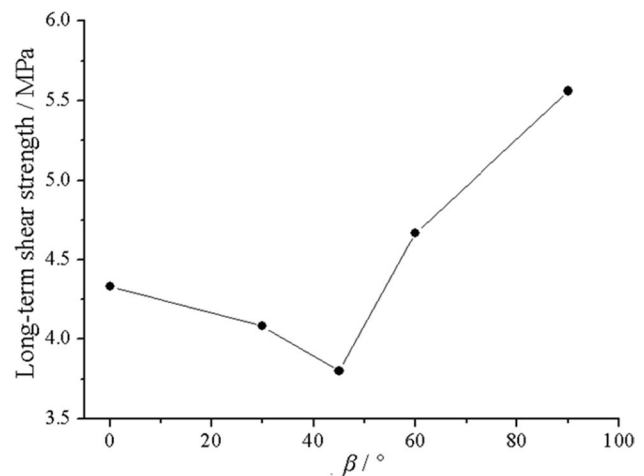
Fig. 5 Variation of the long-term shear strength of the #S4-A60 specimen with the crack dip angle

Fig. 6 Fracture morphology of samples with a fracture length of 40 mm and crack dip angle of 0° and 45°. **a** β is 0°. **b** β is 45°

(a) β is 0°   (b) β is 45°
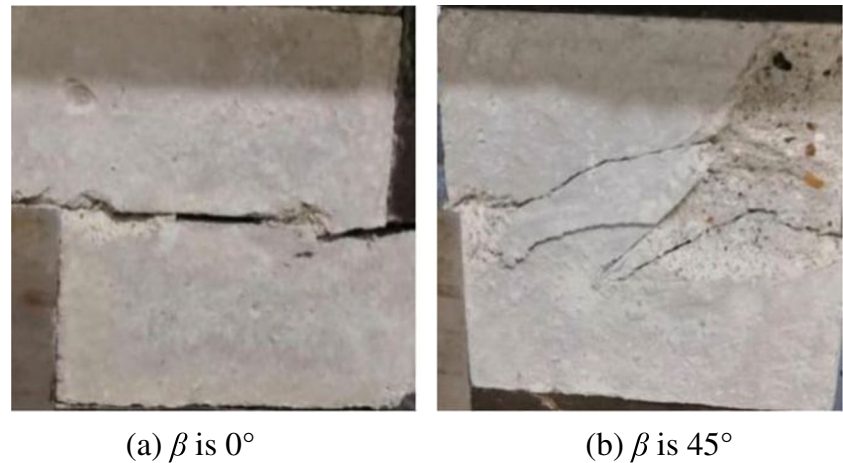
After applying the normal stress at a loading rate of 10 kN/min to the set value (2.5 MPa), the normal stress is kept constant, and the shear stress is applied at the constant rate of 10 kN/min. After applying one level of shear stress for 48 h, the next level is applied until the specimen is sheared and fails. The shear stress increment at each level is 1.2 MPa, and the shear creep test group is shown in Table 1.

The loading steps of shear rheological test are as follows: (1) A normal stress is applied, followed by the addition of shear stress after the positive deformation has stabilized; (2) the shear stress is applied in 3~5 levels until the rock sample undergoes damage; (3) data are collected at regular intervals during the applying a load; (4) the criterion for deformation stability is a shear displacement rate less than 5×10^{-4} mm/day; (5) when the sample is close to fail, careful loading is needed to avoid sudden failure of the rock sample due to excessive loading.

## Analysis of shear creep test results

Analysis of shear creep test curve

Figure 2 shows the shear creep test curve of the sample for different crack dip angles when the crack length is constant at 40 mm. Figure 3 shows the shear creep test curve of the sample for different crack lengths when the crack dip angle is constant at 60°.

After applying the horizontal shear stress, the sample produces instantaneous shear displacement. With an increase in time, the shear displacement gradually increases. After the action of lower horizontal shear stress, the horizontal shear displacement increases rapidly for the next few hours. However, with a further increase in time, the increase rate of the horizontal shear displacement keeps reducing and the creep displacement

Fig. 7 Wing crack of the specimen when the crack length is 40 mm and the crack dip angle is 90°
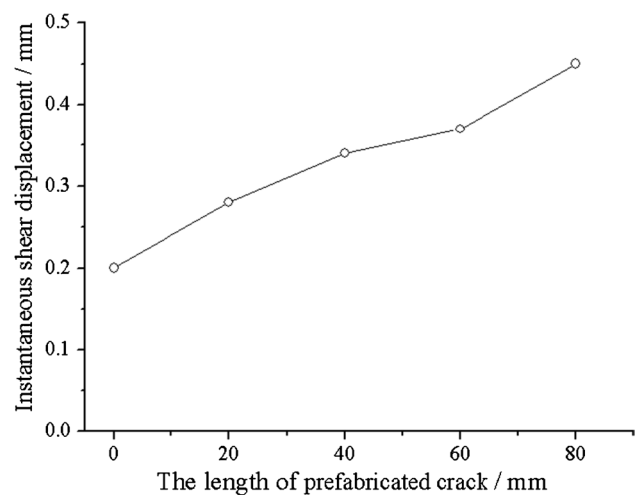
Fig. 8 Effect of the crack length on the instantaneous shear displacement of the specimen when the crack dip angle is 60°

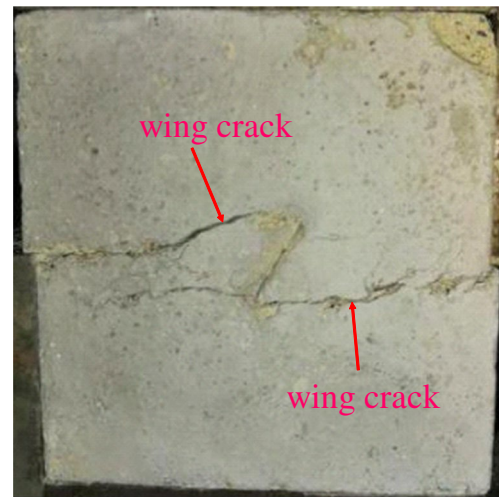Fig. 9 Effect of the crack length on the shear creep displacement of the specimen when the crack dip angle is 60°

Fig. 11 Fracture morphology of the specimen with a crack length of 0 mm
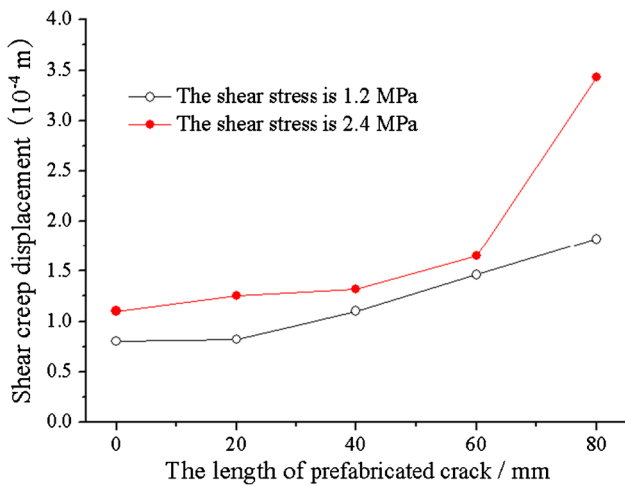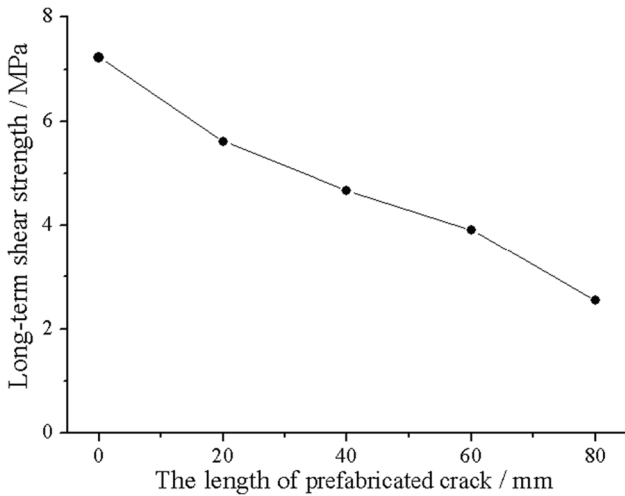
Fig. 10 Effect of the crack length on the long-term shear strength of specimens when the crack dip angle is 60°

Fig. 12 Wing crack of the specimen when the crack dip angle is 60° and the crack length is 20 mm

gradually stabilizes to a certain value. That is, under the action of lower horizontal shear stress, the specimen only shows the decay and stable creep stages. When the horizontal shear stress is high or close to the long-term shear strength of the specimen, the shear displacement creep of the specimen increases significantly and the specimen undergoes the decay, stable, and accelerated creep stages. With an increase in the horizontal shear stress, the shear creep displacement and the average shear creep displacement rate of the specimen increase.
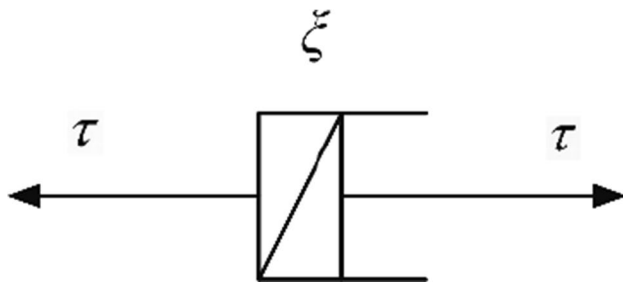
Effect of inclination angle of the crack on the shear creep of specimens

The influence of the inclination angle of the crack on the shear creep displacement of the specimen is shown in Fig. 4.

When the crack length, normal stress, shear stress, and acting time are the same, the shear creep displacement

Fig. 13 Wing crack of the specimen when the crack dip angle is 60° and the crack length is 80 mm
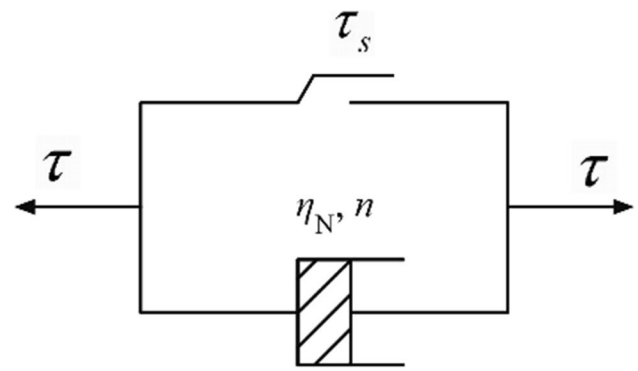

Fig. 14 Software component

Fig. 15 NVPB model

Fig. 16 Nonlinear viscoelastic plastic rheological constitutive model
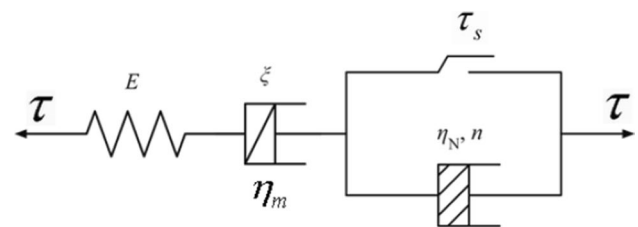
of the sample first increases and then decreases as the inclination angle of the crack increases from 0 to 90°. When the angle is 45°, the shear creep displacement of the sample reaches the maximum value. Furthermore, when the inclination angle of the crack is 90°, the shear creep displacement of the sample attains its minimum value.

The isochronous curve method is used to determine the long-term shear strength of the specimen with cracks. The isochronous curve refers to the curve that represents relationship between creep deformation and stress that corresponds to equal time in a set of creep curves with different stress levels. The isochronous curve of shear stress–shear displacement at various times is obtained from the shear displacement–time relationship curve.

The inflection point of the shear stress–shear displacement isochronous curve reflects the inflection point of the shear displacement of the specimen as the shear stress increases. Moreover, the shear stress corresponding to

this point is the long-term shear strength of the specimen. According to the isochronous curve, the variation law of the long-term shear strength of the #S4-A60 specimen with the crack dip angle is shown in Fig. 5.

When the crack length, normal stress, shear stress, and action time are the same, the long-term strength of the specimen first decreases and then increases with an increase in the crack dip angle from 0 to 90°.

Figure 6 shows the fracture morphology of the sample when the crack length is 40 mm and the crack dip angle is 0° and 45°.

Figure 7 shows the wing crack of the sample when the crack length is 40 mm and the crack dip angle is 90°.

With an increase in shear stress, the stress concentration appears at the tip of the prefabricated crack and at the contact point between the horizontal shear loading plate and the specimen when the crack dip angle is 0°. The crack first appears at both stress concentrations. With a further increase in the shear stress, the crack extends and penetrates the plane in which the prefabricated crack is located, finally inducing damage to the sample. The shear failure plane coincides with the plane of the prefabricated crack. The penetration path of the shear failure crack is clear, and the fracture plane is flat.
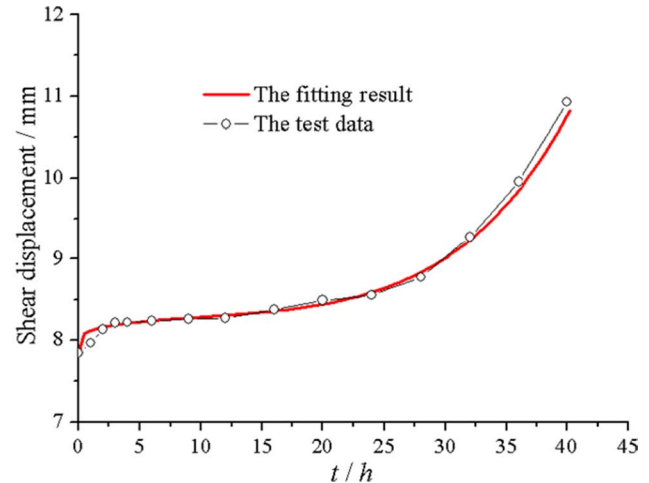
With an increase in the shear stress, the prefabricated crack gradually closes under the action of the shear stress, and the

Table 2 Shear creep parameters of the #S4-A60 specimen under all stress levels

Shear stress (MPa)	G (MPa)	ξ (GPa/h)	β	τ_s (MPa)	η_N (GPa/h)	n
1.2	0.34	21.58	0.21	/	/	/
2.4	0.47	27.63	0.43	/	/	/
3.6	0.56	24.15	0.65	/	/	/
4.8	0.58	8.61	0.24	4.67	2071.26	4.61
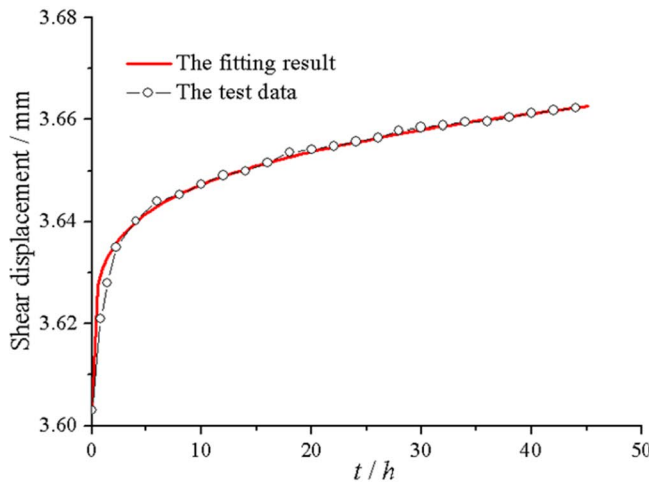
(a) Shear stress is 1.2 MPa

(b) Shear stress is 4.8 MPa

Fig. 17 Comparison results of the test data and theoretical calculation values of the #S4-A60 sample. **a** Shear stress is 1.2 MPa. **b** Shear stress is 4.8 MPa

stress concentration appears at the tip of the prefabricated crack when the crack dip angle is 45° and 90°. The stress concentration also appears at the contact point between the horizontal shear loading plate and the sample. The wing crack still appears at the tip of the prefabricated crack first. With a further increase in the shear stress, the crack propagates to the contact point between the horizontal shear-loaded plate and the specimen, finally causing specimen failure. During shear failure, the shear failure surface is not the central horizontal plane of the specimen, but several groups of failure surfaces appear with the penetration of the main crack.

Effect of the crack length on shear creep of specimens

When the crack dip angle is 60°, the normal stress is 2.5 MPa and the shear stress is 1.2 MPa, the influence of the crack length on the instantaneous shear displacement of the specimen is shown in Fig. 8. The instantaneous shear displacement

of the specimen is the shear displacement generated when the shear stress is applied to a predetermined value.

When the dip angle of the crack is 60°, the normal stress is 2.5 MPa and the shear stress is 1.2 MPa and 2.4 MPa. The influence of the crack length on the shear creep displacement of the specimen is shown in Fig. 9.

When the normal stress and shear stress are the same, and the dip angle of the crack is constant, an increase in the crack length increases the instantaneous shear displacement and shear creep displacement.

The effect of crack length on the long-term shear strength of the specimen is shown in Fig. 10.

When the normal stress and shear stress are the same, and the dip angle of the crack is constant, an increase in the crack length reduces the long-term shear strength of the specimen.

The fracture morphology of the sample when the crack length is 0 mm is shown in Fig. 11. When the crack length is 0 mm, it means that there is no prefabricated crack in the sample.

Figures 12 and 13 show the wing crack of the specimen when the dip angle of the crack is 60° and the crack length is 20 mm and 80 mm.

When there is no prefabricated crack in the sample, with an increase in shear stress level, the location of the initial crack does not have a consistent trend. The shear fracture surface is located close to the central horizontal plane of the specimen but is not smooth. The prefabricated cracks in the specimen gradually close under the action of shear stress. Furthermore, stress concentration and wing cracks appear at the tip of the prefabricated cracks and the contact point between the horizontal shear-loaded plate and the specimen. Therefore, when the dip angle of the crack is constant, the length of the prefabricated crack will not affect the location and propagation form of the crack under the action of shear stress. However, when the crack length is small (20 mm and 40 mm), there are multiple cracks after the specimen is damaged, several blocks of specimen fall off, and the specimen is relatively broken. When the crack length is large (60 mm and 80 mm), the final fracture surface of the sample is close to the central horizontal plane and the fractured sample is relatively intact.

Creep model and parameter identification

Yin et al. (2007) proposed a software element based on fractional calculus theory (Fig. 14), and its mechanical property is between ideal solid and ideal fluid.

The shear creep equation of the software component is as follows:

$$u(t) = \frac{\tau}{\xi} \frac{t^\beta}{\Gamma(1+\beta)} \quad (0 \le \beta \le 1) \tag{1}$$

where $\Gamma(1 + \beta)$ is the gamma function. $u(t)$ is the shear displacement. T is time. τ is the shear stress. β is the order of fractional order differentiation. ξ is the viscoelasticity coefficient. The expression for $\Gamma(\beta)$ is given as follows:

$$\Gamma(\beta) = \int_0^\infty t^{\beta-1} e^{-t} dt \tag{2}$$

Xu et al. (2005) proposed a nonlinear element connected in parallel with the plastic body to form an nonlinear viscoplastic body (NVPB) model that can reflect the accelerated creep of rocks (Fig. 15).

The shear creep equation is as follows:

$$u(t) = \frac{H(\tau - \tau_S)}{\eta_N} = \frac{t^n}{t_0^{n-1}} = \frac{H(\tau - \tau_S)}{\eta_N} t^n \tag{3}$$

Here, n represents the creep index of the material, η_N represents the viscosity coefficient of the material,

t_0 represents the reference time, and the initial value of t_0 is 1. τ_S is long-term shear strength. The function of $H(\tau - \tau_S)$ can be expressed by Eq. (4):

$$H(\tau - \tau_S) = \begin{cases} 0 & \tau < \tau_S \\ \tau - \tau_S & \tau \ge \tau_S \end{cases} \tag{4}$$

In this study, the software component shown in Fig. 14 is used to replace the dash pot in the Maxwell model and is connected in series with the NVPB model proposed by Xu et al. (2005) to obtain a new nonlinear viscoelastic plastic rheological model (Fig. 16).

The shear creep equation is as follows:

$$u(t) = \frac{\tau}{G} + \frac{\tau}{\xi} \frac{t^\beta}{\Gamma(1+\beta)} \quad \tau < \tau_s \tag{5a}$$

$$u(t) = \frac{\tau}{G} + \frac{\tau}{\xi} \frac{t^\beta}{\Gamma(1+\beta)} + \frac{\tau - \tau_s}{\eta_N} t^n \quad \tau \ge \tau_s \tag{5b}$$

where G is the elastic shear modulus.

When fitting the shear creep test curve and the shear stress does not exceed the long-term strength of the sample, the corresponding expression (Eq. 5a) is used for fitting. When the shear stress exceeds the long-term strength of the sample, the corresponding expression (Eq. 5b) is used for fitting. Here, the shear creep curves of the #S4-A60 specimen under various levels of shear stress are fitted, and their creep parameters are shown in Table 2. The comparison between the test and theoretical calculation results is shown in Fig. 17.

The fitting curve is consistent with the laboratory creep test curve, indicating that the nonlinear viscoelastic plastic creep model is suitable for describing the shear rheological properties of rock-like specimens with an accelerated creep stage.

Conclusions

By conducting shear creep tests on actual rock-like samples and those with cracks, the following conclusions were obtained:

(1) The shear creep displacement and the average shear creep displacement rate of the specimen increase with the increase of the horizontal shear stress when the crack dip angle, crack length, and normal stress are the same.

(2) The shear creep displacement of the specimen first increases and then decreases, and the long-term strength of the specimen first decreases and then increases, with an increase in the crack dip angle from 0 to 90° when the crack length, normal stress, shear stress, and creep time are the same.

(3) When the normal stress, the shear stress, and the dip angle of the crack are the same, an increase in the crack length increases the instantaneous shear displacement and shear creep displacement and reduces the long-term shear strength.

(4) During the shear creep test, cracks first appeared at the tip of the prefabricated crack and then extended to the contact point between the specimen and the horizontally loaded plate. When the crack dip angle is constant, an increase in the crack length reduces the cracks in the specimen in the final failure, and the specimen remains relatively intact.

(5) A new nonlinear viscoelastic plastic creep model is used to fit the shear creep experimental curve. The results show that the fitting curve is consistent with the experimental curve, indicating the rationality of the model.

Declarations

Conflict of interest The authors declare no competing interests.

References

Chen YJ, Wu C, Fu YM (2008) Rheological characteristics of soft rock structural surface. J Cent South Univ Technol 15:374–380

Jia CJ, Xu WY, Wang RB, Wang SS, Lin ZN (2018) Experimental investigation on shear creep properties of undisturbed rock discontinuity in Baihetan Hydropower Station. Int J Rock Mech Min Sci 104:27–33

Li P, Liu J, Zhu JB, He HJ (2008) Research on effects of water content on shear creep behavior of weak structural plane of sandstone. Rock and Soil Mechanics 29:1865–1871 (In Chinese)

Shen MR, Zhang QZ (2008) Study on creep characteristics of regular rock mass discontinuity. Chin J Rock Mech Eng 27:3793–3797 (In Chinese)

Shen MR, Zhang QZ (2010) Study of shear creep characteristics of greenschist discontinuities. Chin J Rock Mech Eng 29:1149–1155 (In Chinese)

Shen MR, Zhu GQ (2004) Testing study on creep characteristic of regularly dentate discontinuity. Chin J Rock Mech Eng 23:223–226 (In Chinese)

Shen MR, Chen HJ, Zhang QZ (2012) Method for determining long-term strength of discontinuity using shear creep test. Chin J Rock Mech Eng 31:1–7 (In Chinese)

Xu WY, Yang SQ (2005) Experiment and modeling investigation on shear rheological property of joint rock. Chin J Rock Mech Eng 24:5536–5542 (In Chinese)

Xu WY, Yang SQ, Xie SY, Shao JF, Wang YF (2005) Investigation on triaxial rheological mechanical properties of greenschist specimen (II): model analysis. Rock and Soil Mechanics 26:693–698 (In Chinese)

Yan ZJ, Xia CC, Wang XD, Zhang CS (2009) Shear rheological properties and model for rock joints. J Tongji Univ (Natural Science) 37:601–606 (In Chinese)

Yang SQ, Xu WY, Yang SL (2007) Investigation on shear rheological mechanical properties of shale in Longtan Hydropower Project. Rock Soil Mech 28:895–902 (In Chinese)

Yin DS, Ren JJ, He CL (2007) Chen W (2007) A new rheological model element for geomaterials. Chin J Rock Mech Eng 26:1899–1903 (In Chinese)

Zhang ZL, Xu WY, Zhao HB, Jian B (2010) Investigation on shear creep experiments of sandstone with weak plane in XiangJiaBa Hydropower Station. Chin J Rock Mech Eng 29:3693–3698 (In Chinese)

Zhang QZ, Shen MR, Ding WQ (2011a) Study on the shear creep characteristics and constitutive model of rock mass discontinuity. Chin Civil Eng J 44:127–132 (In Chinese)

Zhang QZ, Shen MR, Wen Z (2011b) Investigation of mechanical behavior of a rock plane using rheological tests. J Mater Civ Eng 23:1220–1226

Zhang QZ, Shen MR, Ding WQ, Clark C (2012) Shearing creep properties of cements with different irregularities on two surfaces. J Geophys Eng 9:210–217